





 Cite this: *RSC Adv.*, 2025, 15, 37474

Synthesis of borylated-stilbenes under environmentally friendly Wittig reaction and interaction studies with HSA

 Pedro H. V. Vontobel, Eduam O. Boeira,  Jessie S. da Costa, Legna Colina-Vegas  and Angélica V. Moro *

Herein we report the Wittig reaction conducted under environmentally friendly conditions for the synthesis of borylated analogues of resveratrol. For the synthesis of analogues featuring the boronic ester functional group, we developed a micellar aqueous method that yielded borylated-stilbenes in good yields with a low diastereomeric ratio. To circumvent this low selectivity, we employed an isomerization reaction, which provided borylated stilbenes with high selectivities ($\geq 95:05$). For synthesizing analogues containing the benzoxaborole and boronic acid functional groups, a biphasic toluene-water system emerged as the optimal reaction medium. Three functionalized stilbenes-bearing boronic ester, benzoxaborole, and boronic acid interact with a single binding site on HSA, with the benzoxaborole derivate exhibiting the highest affinity. Based on thermodynamic analysis, boronic ester and the benzoxaborole derivate bind to HSA *via* hydrophobic interactions, whereas the boronic acid derivate binds *via* electrostatic forces.

Received 17th July 2025

Accepted 23rd September 2025

DOI: 10.1039/d5ra05162b

rsc.li/rsc-advances

Introduction

Human serum albumin (HSA), the most abundant protein in blood plasma, plays a crucial role in the transport and distribution of various biological and pharmacological species, such as nutrients, fatty acids, steroids, and many commonly used drugs like warfarin and ibuprofen.¹ The abundance of HSA in the blood plasma together with its extraordinary binding capabilities make it an important tool in the development of novel drugs.² Drug delivery to cells may be facilitated through binding to serum albumin and improving its solubility. Hence plasma protein binding has been considered as one of the most important physicochemical characteristics of drugs that can alter their pharmacokinetics and pharmacodynamics.³ Achieving information on the nature of drug-HSA interaction provides a better understanding for its use and can suggest new approaches to structural modifications.

Resveratrol is a natural stilbene found in grapes and consequently in red wine (Fig. 1).⁴ This bioactive polyphenol exhibits many functional properties, including antioxidant, anti-inflammatory, neuro- and cardioprotective, anticarcinogenic, anti-aging, anti-diabetic, and anti-obesity properties.⁵ The distribution of resveratrol in humans and its therapeutic applications are affected by its low solubility in water (0.023 mg mL⁻¹), low oral bioavailability, tendency to undergo oxidation and high photosensitivity in aqueous media.⁶ HSA plays

a fundamental role in the distribution and bioavailability of resveratrol in the bloodstream, and protection from the degradative effects of radiation.⁷ However, the HSA binds resveratrol only when its concentration is high.⁸ Therefore, significant efforts have been made for the development of technologies or analogues that overcome these limitations. The methoxylated analogues of resveratrol possess increased lipophilicity and a pharmacological profile comparable or even superior to that of resveratrol.⁹ Among them, DMU-212 has disclosed a strong anti-cancer activity with higher chemoprotective activity than resveratrol. In this regard, the synthesis of boronated analogues of resveratrol present an interesting alternative, especially after the FDA approval of bortezomib and ixazomib for multiple myeloma treatment, crisaborol for atopic dermatitis treatment, vaborbactam for urinary tract infection treatment, and tavaborole for onychomycosis treatment. Some synthesized boronated analogues of resveratrol already exhibit activity as inhibitor human cancer cells and lipogenic inhibitor in mammalian hepatocytes (Fig. 1).¹⁰

A Wittig reaction is a widely used method for the synthesis of stilbenes.¹¹ However, when applied to the synthesis of boronated analogues of resveratrol, the reaction is conducted in the presence of strong bases (such as *t*BuONa or *n*BuLi) and DMF or THF as the solvent (Scheme 1a).¹² In this case, the use of the traditional Wittig condition has been applied to a limited number of substrates, and with the boron functionality placed at the same position (*para*). The reported examples typically result in low to moderate *E/Z* selectivity which requires separation of diastereoisomers when they are necessary for biological studies. Based on our research group's experience in

Institute of Chemistry, Universidade Federal do Rio Grande do Sul, Av. Bento Gonçalves 9500, Porto Alegre, RS, 91501-970, Brazil. E-mail: angelica.venturini@ufrgs.br; Fax: +55 51 3308 9637



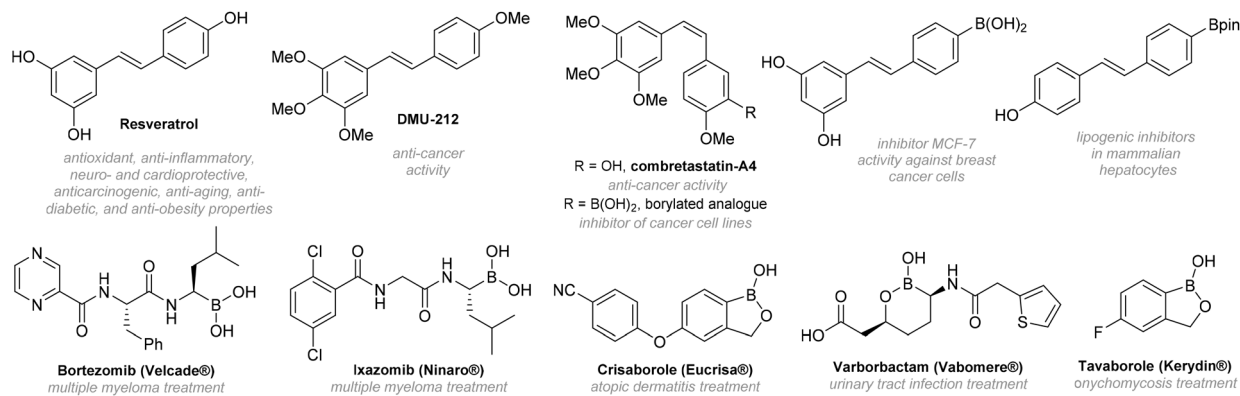
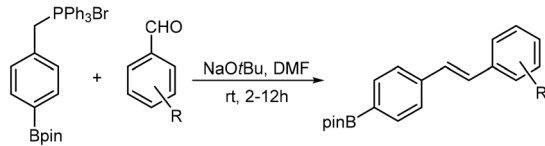
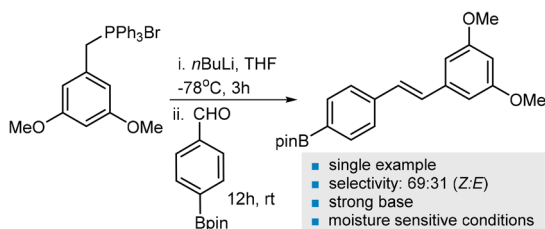


Fig. 1 Examples of biologically active stilbenes (top) and FDA-approved boron-containing drugs (bottom).

(a) Traditional Wittig

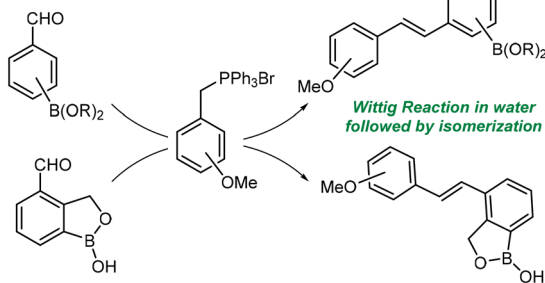


- 15 examples containing boron exclusively at the *para* position
- low to moderate selectivity in most cases
- good yields for electron-donating and electron-withdrawing substituents
- strong base, toxic solvent and inert atmosphere



- single example
- selectivity: 69:31 (Z:E)
- strong base
- moisture sensitive conditions
- toxic and dry solvent

(b) This work



- 16 boronated analogues of resveratrol and DMU-212
 - different boron species at different positions
 - mono, di or tri-methoxylated compounds
 - green solvents and simple reactions conditions
 - moderate to good yields and high diastereoselectivity after isomerization
- up to 95:05 (E:Z)

Scheme 1 (a) Traditional Wittig approach and (b) this work.

conducting organic reactions in aqueous or more environmentally friendly media,¹³ we directed our efforts to improving the conditions used in the Wittig reaction for boron-functionalized stilbenes, especially towards their study for interaction with HSA protein, which required the compounds to be stereochemically pure.

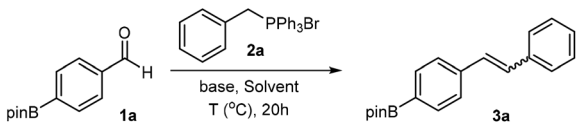
Inspired by the bioactive structures of resveratrol and its analogue DMU-212, our main focus was to develop a synthetic method for *E*-stilbenes featuring one, two, or three methoxy groups on one aryl ring, and various boron-containing functional groups positioned differently on the second ring (Scheme 1b).

Results and discussion

To investigate the optimal conditions for the Wittig reaction, the selected model substrates were aldehyde **1a**, which contains a boronic ester group in the *para*-position, and phosphonium salt **2a**. The initial conditions evaluated were based on previous studies that conducted Wittig reactions in aqueous systems with non-functionalized boron substrates. In the work by Ismael and coworkers,¹⁴ which employed NaOH in a biphasic CH₂Cl₂/H₂O system, the boron-containing Wittig product **3a** was obtained with a yield of 63%, favoring the *Z*-isomer at a 36 : 64 ratio (Table 1, entry 1). Using the methodology described by Wu and collaborators,¹⁵ which involves an aqueous solution of LiCl and NaOH, the product **3a** was obtained with a 39% yield and a 33 : 67 ratio favoring the *Z*-isomer (entry 2). Conducting the reaction without LiCl and any organic solvent resulted in an increased yield (entry 3). However, a decrease in yield was noted when ethanol was used as a solvent (entry 4). Inspired by the work of Orsini and coworkers, sodium dodecyl sulfate (SDS) was employed as a surfactant in water for the Wittig reaction, but this resulted in a low yield (entry 5). Switching the surfactant to SPGS-550M¹⁶ allowed for the isolation of a mixture of diastereoisomers **3a** with a yield of 57% (entry 6). In contrast, using TPGS-750M¹⁷ as a surfactant resulted in a high yield of 89% for the desired product **3a** (entry 7). TPGS-750 M has a larger micelle size (50–100 nm) compared to SPGS-550 M (40–60 nm), which may have better accommodated the bulky reagents, thus enhancing reaction efficiency within the micelle.

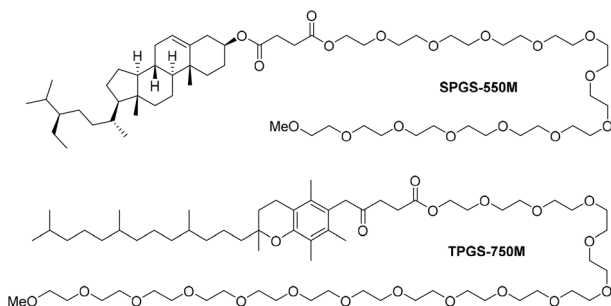
Subsequently, the effects of phosphonium salt stoichiometry and reaction temperature were evaluated. Reducing the amount of phosphonium salt from 1.5 to 1.1 equivalents, resulted in a decrease in yield to 47% (entry 8). Lowering the temperature to 25 °C and 60 °C caused a significant drop in yield (entries 9 and 10). Finally, weaker bases were evaluated, considering that more



Table 1 Optimizations of the Wittig reaction using **1a** and **2a**


Entry ^a	Base	T (°C)	Solvent	E : Z ^b	Yield ^c (%)
1 ^d	NaOH	100	CHCl ₃ /H ₂ O (2 : 1)	36 : 64	63
2	NaOH	100	H ₂ O/LiCl 1.4 M	33 : 67	39
3	NaOH	100	H ₂ O	36 : 64	67
4 ^c	NaOH	100	EtOH	46 : 56	47
5	NaOH	100	H ₂ O/SDS 10%	41 : 59	37
6	NaOH	100	H ₂ O/SPGS-550M 2%	40 : 60	57
7	NaOH	100	H₂O/TPGS-750M 2%	48 : 52	89
8 ^e	NaOH	100	H ₂ O/TPGS-750M 2%	46 : 54	47
9	NaOH	25	H ₂ O/TPGS-750M 2%	53 : 47	42
10	NaOH	60	H ₂ O/TPGS-750M 2%	47 : 53	45
11	K ₂ CO ₃	100	H ₂ O/TPGS-750M 2%	46 : 54	63
12	Et ₃ N	100	H ₂ O/TPGS-750M 2%	46 : 54	67
13	DIPEA	100	H ₂ O/TPGS-750M 2%	42 : 58	37

^a Using **1a** (1.0 mmol), **2a** (1.5 mmol), base (1.5 mmol) in solvent (2 mL), 24 h. ^b The E : Z ratio determined by the proportion of Bpin methyl signals in the ¹H NMR spectrum. ^c Isolated yields after treatment with ZnCl₂ and purification by column chromatography. ^d Reaction carried out in a sealed tube. ^e 1.1 equivalent of the phosphonium salt were used.



reactive boron species with a higher tendency for protodeboronation in basic conditions would be investigated later. The use of K₂CO₃ and Et₃N (entries 11 and 12) yielded moderate results of 63% and 67%, respectively, while DIPEA produced a lower yield of 37% (entry 13). Across all evaluated reactions, there was no significant preferential formation of a single diastereoisomer.

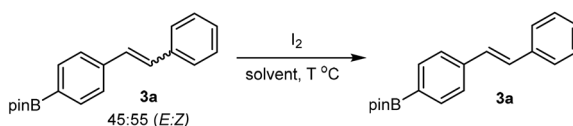
The Wittig reaction has the disadvantage of producing triphenylphosphine oxide (OPPh₃) as a by-product during the formation of the C=C bond. This oxide complicates the purification of the Wittig product and was removed from the crude reaction mixture by treatment with ZnCl₂ in ethanol, which leads to the precipitation of the complex ZnCl₂(OPPh₃)₂, removed by filtration. After this treatment, the mixture of stereoisomers **3a** was purified by column chromatography, resulting in the separation of the E and Z stereoisomers. The differentiation of the E and Z diastereoisomers was performed using the ¹H NMR analyses, considering the chemical shifts of the olefinic hydrogens and their coupling constants.

After obtaining the Wittig products as a mixture of diastereoisomers, different isomerization conditions were studied to favor the E isomer as the major product. The studies were conducted according to the method of Ismail and coworkers,¹⁴ which involves the isomerization of stilbenes with I₂ in hexane under reflux (Table 2). Under the evaluated conditions, a strong dependence on temperature was observed in the performance of the reaction when it was changed from 40 to 100 °C, using a series of halogenated solvents (Table 2, entries 1–4). The higher the reaction temperature, the greater the ratio of the E isomer obtained at the end. The reaction at 100 °C in dichloroethane yielded the E isomer in a ratio of ≥95 : 5 (entry 4). When the solvent was changed to more environmentally friendly options, such as ethanol, ethyl acetate, and water with and without the presence of TPGS-750 M, the E isomer was obtained in high yields and diastereomeric ratios (entries 5–8).

Notably, the products were obtained in good purity without the need for additional purification. Considering that both the Wittig reaction and isomerization can be performed in water, an attempt was made to carry them out in a one-pot manner. Performing the Wittig reaction in water/TPGS-750 M at 100 °C with the addition of I₂, with or without ZnCl₂, did not result in efficient isomerization, and stilbene **3a** was obtained as a mixture of diastereoisomers. No improvement was observed with the addition of toluene as a co-solvent.

Despite the high yield and selectivity for the isomerization of **3a** in water, when applied to other substrates, there were difficulties in solubilizing most of the compounds, which drastically affected the yield of the isomerization. Therefore, ethyl acetate was the chosen solvent for the isomerization, leading to high yields and selectivities for the desired stilbenes (Scheme 2).

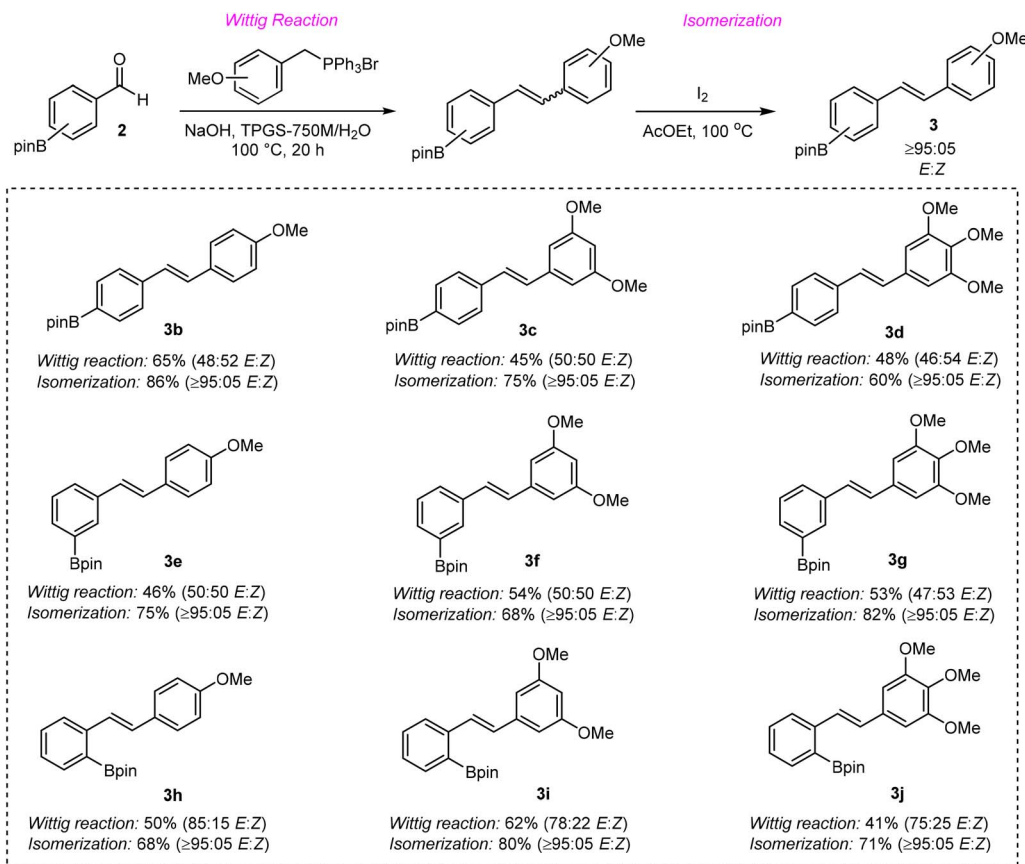
Aldehydes containing boronic ester groups in the *para*-, *meta*-, and *ortho*-positions were subjected to reaction in a micellar aqueous medium with phosphonium salts containing 1, 2, or 3 methoxy groups. For the *para*- and *meta*-substituted

Table 2 Optimizations of isomerization using **3a**


Entry	Solvent	T (°C)	E : Z final ^b	Yield ^a (%)
1	CH ₂ Cl ₂	40	45 : 55	72
2	CHCl ₃	60	45 : 55	70
3	ClCH ₂ CH ₂ Cl	85	86 : 14	79
4 ^c	ClCH ₂ CH ₂ Cl	100	≥95 : 05	82
5	H ₂ O	100	≥95 : 05	82
6 ^d	H ₂ O	100	91 : 09	84
7 ^c	EtOH	100	92 : 08	90
8 ^c	AcOEt	100	≥95 : 05	86

^a Yields without column chromatography purification. ^b The E : Z diastereomeric ratio was determined by ¹H NMR from the Bpin methyl signals in the spectrum. ^c Reaction conducted in a sealed tube. ^d TPGS-750 M 2% used as a surfactant.



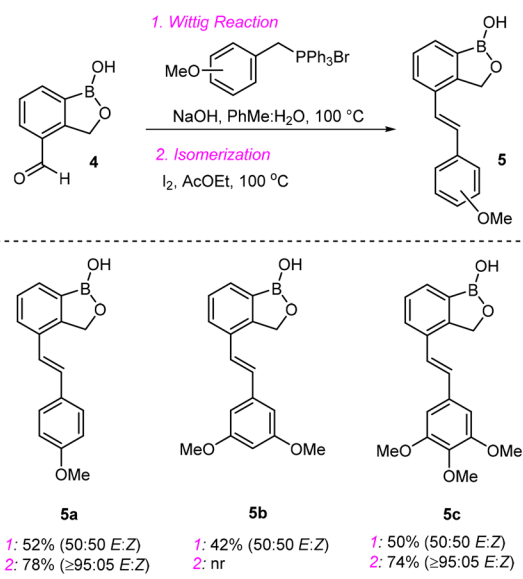


Scheme 2 Wittig products bearing boronic esters.

aldehydes with boronic ester, there was no selectivity favoring one of the isomers in the Wittig reaction. However, for the *ortho*-substituted aldehydes with boronic ester, the formation of the *E* isomer predominated (examples **3h**, **3i**, and **3j**), particularly for compound **3h**, which exhibited a selectivity of 85 : 15. The yields for all reactions were moderate to good, ranging from 41% to 65%. All isomerizations were effective, providing products with high diastereoselectivity ($\geq 95 : 05$) in favor of the *E* isomer. The developed methodology was applied to the aldehyde containing the benzoxaborole core **4**, resulting in the cleavage of the C–B bond and the formation of the protodeboronation product. After a brief study of this reaction, it was observed that in a micellar aqueous medium, protodeboronation occurred rapidly. Subsequently, other solvents and biphasic systems were evaluated, and it was found that protodeboronation did not occur using the biphasic toluene and water system (Scheme 3). Consequently, under these conditions, three derivatives containing the benzoxaborole core were synthesized in moderate yields (**5a**, **5b** and **5c**). Finally, isomerization was performed, allowing the synthesis of compounds **5a** and **5c** with high diastereoselectivity. However, adduct **5b** proved resistant to the isomerization process, maintaining an *E* : *Z* ratio of 50 : 50.

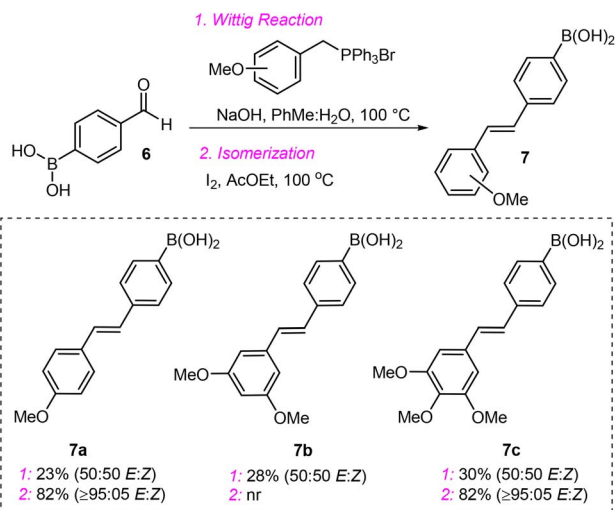
The biphasic toluene and water system were also used for the reaction of boronic acid-containing aldehyde **6** (Scheme 4). The yields obtained were low, ranging from 23% to 30%, for the three synthesized compounds **7a–c**. The isomerization step

occurred with high yield and high diastereoselectivity for compounds **7a** and **7c**. Once again, isomerization failed for the substrate **7b**, which does not contain an electron-donating group at the *para* position of the ring. It is worth noting that,



Scheme 3 Wittig products bearing benzoxaborole.

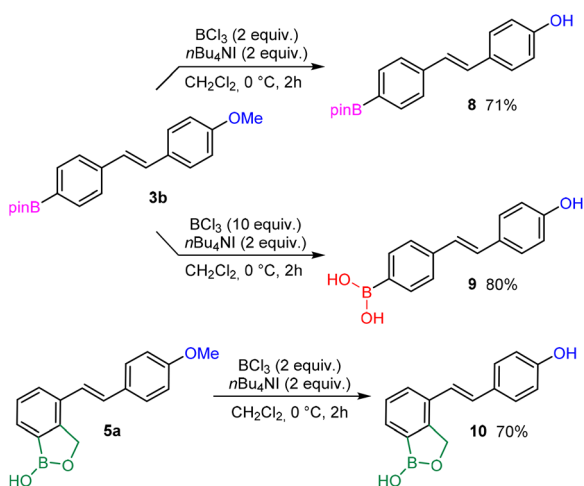




Scheme 4 Wittig products bearing boronic acid.

despite the low yields of the Wittig reaction for boronic acid-functionalized substrates, no examples were found in the literature of Wittig reactions with these free groups, without the presence of pinacol as protecting group.

The Wittig reaction did not tolerate the presence of phosphonium salts containing a free hydroxyl group, regardless of whether the reaction was conducted in a micellar aqueous medium or an organic solvent. Due to the incompatibility of the developed methodology for the Wittig reaction with a phosphonium salt containing a free hydroxyl group, hydroxylated analogs of resveratrol were synthesized through the demethylation of the previously obtained methoxylated compounds (Scheme 5). The first methodology evaluated used AlCl_3 and pyridine in toluene under reflux; however, the starting material was not consumed in the process. Demethylation was efficient when BCl_3 and $n\text{Bu}_4\text{NI}$ were used in dichloromethane at 0 °C, yielding the demethylated products **8** and **10** with 71% and 70% yield, respectively. By using an excess of $\text{BCl}_3/n\text{Bu}_4\text{NI}$, it was

Scheme 5 Demethylation and deprotection of **3b** and **5a**.

possible to carry out the demethylation and the removal of the pinacol in a single step, resulting in the formation of **9** with an 80% yield. It's worth to point out that this strategy allowed us to prepare three phenolic derivatives with different organoboron functionalities, boronic ester, boronic acid, and benzoxaborole.

The interaction between HSA and three functionalized boronic ester (**3b**), benzoxaborole (**5a**) and boronic acid (**7a**) was investigated using tryptophan fluorescence quenching experiments. HSA was prepared in Tris-HCl buffer (4.5 mM Trizma HCl, 0.5 mM Trizma Base and 50 mM NaCl) and the intrinsic fluorescence of its tryptophan residues was monitored using a Cary Eclipse fluorescence spectrophotometer. The concentration of HSA in the samples was maintained constant at 2.5 μM , while the quencher concentrations were varied from 1, 2.5, 5, 10, 15, 20, 25, to 30 μM using 10% dimethylsulfoxide. After sample preparation, the solutions were incubated in a water bath for 24 h at 300 K or 310 K. Fluorescence intensity values were measured in triplicate for each concentration. Upon excitation at 270 nm, fluorescence emission spectra were recorded at 300–500 nm.

The tryptophan 217 residue is largely responsible for the fluorescence of HSA, with minor contribution of tyrosine and phenylalanine residues.¹⁸ Organic and inorganic compounds can act as substrate binding to HSA altering its intrinsic fluorescence, inducing conformational changes in the structure. The binding constant force and the thermodynamic nature of these interactions can be elucidated by mathematical models.

Pioneering studies by Sudlow in 1975 and 1976, identified two specific binding sites on HSA known as: site I and site II, referred to as the warfarin and benzodiazepine binding sites, respectively.^{19,20} Site I typically binds substrates containing carboxylic acids or bulky heterocycles with a negative charge at the center of the structure. It is also described as having a broad and flexible region, capable of accommodating a wide range of ligands, including multiple ligands simultaneously. For the other hand, the site II is predominantly a hydrophobic cavity, with only a small polar region containing the residues tyr-411 and arg-410. This characteristic makes the site II more likely to bind structures with carboxylic acids at one end, separated from hydrophobic fragments.²¹

The fluorescence spectra revealed a gradual reduction in the intrinsic fluorescence of HSA at 330 nm as the increased concentration of the studied compounds **3b**, **5a** and **7a** (Fig. 2). The fluorescence decay followed a linear pattern with increasing concentrations of the boronic acid, while an exponential decay pattern was observed for the boronic ester and benzoxaborole. Notably, the benzoxaborole and boronic ester compounds displayed fluorescence emission maxima at 379 nm and 435 nm, respectively. The fluorescence emission pattern of the compounds is similar in the absence of HSA, indicating that the observed spectra does not result from any interaction of the compounds with the protein.

The Stern-Volmer equations along with their corresponding graphs (Fig. 3), were employed to investigate the interaction between each compound and HSA.



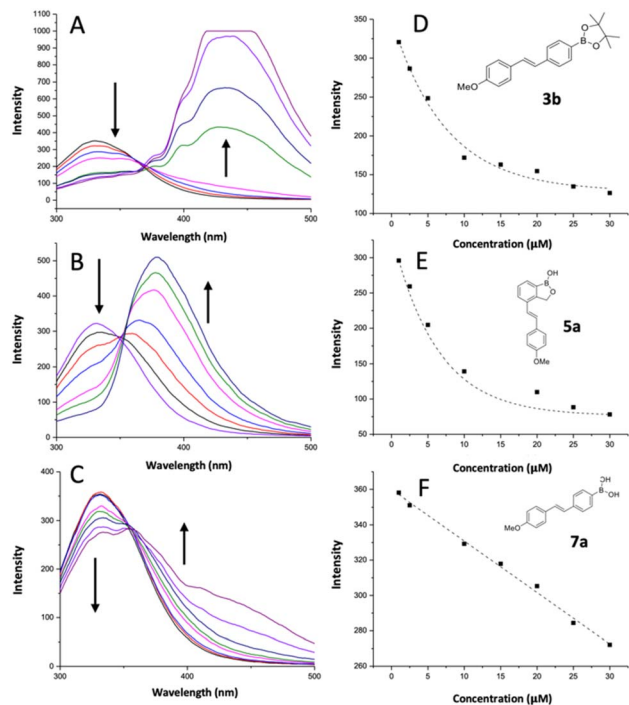


Fig. 2 (A–C) Fluorescence spectra ($\lambda_{\text{ex}} = 270$ nm) of HSA were recorded in the presence of the compounds at concentrations ranging from 1 to 30 μM , prepared in a solution of 10% v/v DMSO in water and Tris–HCl buffer (pH = 7.4). (D–F) The fluorescence decay pattern of HSA at 330 nm was analysed as a function of increasing compound concentrations.

$$\frac{F_0}{F} = k_q \tau_0 [Q] + 1 = K_{\text{sv}} [Q] + 1 \text{ (Stern–Volmer equation)}$$

where F_0 and F are the fluorescence intensity in the absence and presence of the quencher, K_{sv} is the Stern–Volmer constant, $[Q]$ is the concentration of the quencher, k_q is the fluorescence quenching rate, and τ_0 is the fluorescence half-life of the protein in the absence of the quencher.

$$\log\left(\frac{F_0 - F}{F}\right) = \log K_b + n \log [Q]$$

where K_b is the binding constant and n the number of binding sites. These analyses of the van't Hoff were used also to calculate the thermodynamic parameters ΔH^0 and ΔS^0 .

$$\ln\left(\frac{K_{bT_2}}{K_{bT_1}}\right) = \left(\frac{1}{T_1} - \frac{1}{T_2}\right) \frac{\Delta H}{R} \text{ (van't Hoff equation)}$$

where the values of K_{bT_2} and K_{bT_1} correspond to the binding constants at temperatures at T_2 (310 K) and T_1 (298 K); R is the universal gas constant.

Furthermore, the change ΔG was calculated from the following equation: $\Delta G = -RT \ln K_b = \Delta H - T\Delta S$. All values for compound–HSA systems at different temperatures are summarized in the Table 1. The K_{sv} values obtained at 300 and 310 K for **5a** indicate an inversely proportional relationship, suggesting a static fluorescence quenching mechanism. This implies the formation of a non-fluorescent adduct between HSA

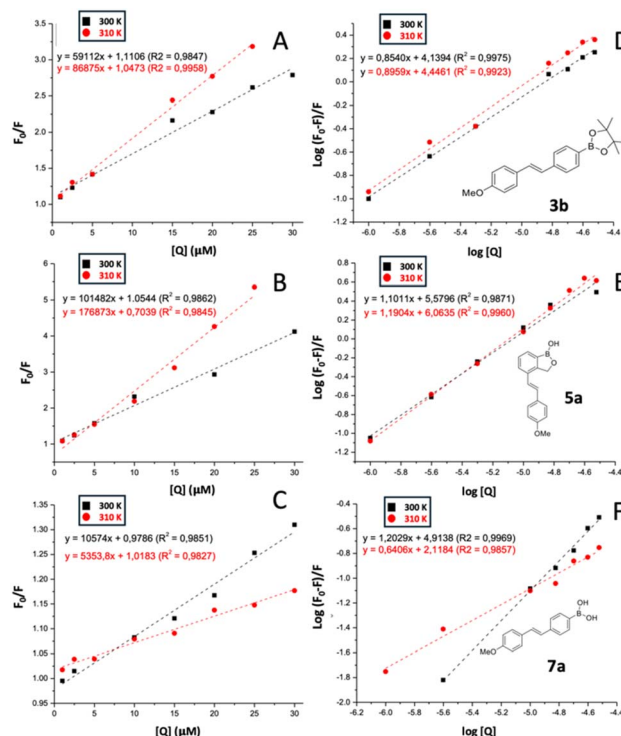


Fig. 3 (A–C) Stern–Volmer plots (F_0/F vs. $[Q]$) for fluorescence quenching and (D–F) Double logarithmic plots ($\log((F_0 - F)/F)$ vs. $\log [Q]$) at two temperatures, generated from the fluorescence decay of HSA at 330 nm.

and the boronic acid, which accounts for the observed phenomenon. In contrast, the K_{sv} values for **3b** and **5a** show a directly proportional relationship with temperature, indicating a dynamic fluorescence quenching mechanism driven by molecular collisions.²²

It was observed that the three compounds tend to interact with a single binding site (n) on HSA at both temperatures with a range value of n between 0.6 to 1.2 (Table 3). The binding constants K_b revealed that the benzoxaborole **5a** exhibits a higher affinity for HSA compared to the boronic ester **3b** and the boronic acid **7a**. Additionally, for **3b** and **5a**, an increase in temperature led to a rise in the binding constant K_b suggesting that their association with HSA is an endothermic process. In contrast, for the compound **5a**, the binding constant K_b decreased with increasing temperature, indicating an exothermic interaction. Ross *et al.* propose three predominant

Table 3 Stern–Volmer Quenching constant (K_{sv} , M^{-1}), biomolecular binding constant (K_b , M^{-1}), number of binding sites (n), ΔG (kJ mol^{-1}), ΔH (kJ mol^{-1}), and ΔS ($\text{J mol}^{-1} \text{K}^{-1}$) compound–HSA systems at different temperatures

	T (K)	$K_{\text{sv}} \times 10^4$	$K_b \times 10^4$	n	ΔG	ΔH	ΔS
3b	300	5.91	1.53	0.8	−23.8	0.65	82.1
	310	8.69	3.11	0.9	−26.6		83.3
5a	300	10.1	13.9	1.1	−29.3	1.96	105.1
	310	17.7	115	1.2	−35.9		122.4
7a	300	1.05	8.20	1.2	−28.0	−5.82	74.5
	310	0.53	0.01	0.6	−12.9		22.9



modes of interaction based on thermodynamic parameter values: hydrophobic interactions ($\Delta H > 0$ and $\Delta S > 0$), van der Waals forces or hydrogen bonding ($\Delta H < 0$ and $\Delta S < 0$), and electrostatic forces ($\Delta H < 0$ and $\Delta S > 0$).²³

For boronic ester **3b** and the benzoxaborole **5a**, the thermodynamic parameters indicate that the driving force for their association with HSA is related to an increase in the system's entropy. The ΔH values for both compounds suggest an endothermic association with HSA, consistent with the temperature-dependent increase in their binding constants K_b . According to Ross's proposal, the predominant interaction mode between HSA and **3b** or **5a** is through hydrophobic interactions.

In the case of the boronic acid **7a**, its association with HSA is governed by both the exothermic nature of the reaction and an increase in entropy. The ΔH value indicates an exothermic association, aligning with the temperature-dependent decrease in its binding constant K_b . Based on Ross's proposal, the predominant interaction mode between HSA and the boronic acid **7a** is through electrostatic forces.

The interaction between boronic acid derivatives and bovine serum albumin (BSA) can significantly enhance fluorescence and binding affinity, as demonstrated previously by the complexation of phenylboronic acid (PBA) with 2-(2-hydroxyphenyl)benzimidazole (HPBI). This complexation not only enhances the fluorescence of the enol form of HPBI but also increases its affinity for proteins. For instance, the binding constant of free HPBI to BSA ($2 \times 10^4 \text{ M}^{-1}$) increases dramatically to $1.2 \times 10^6 \text{ M}^{-1}$ when HPBI is complexed with benzoxaborole. This phenomenon highlights the potential of boronic acid derivatives for non-covalent protein interaction or bioconjugation.²⁴

Conclusions

In conclusion, this study successfully synthesized borylated analogues of resveratrol *via* the Wittig reaction under environmentally friendly conditions. A micellar aqueous method produced borylated stilbenes with good yields, followed by isomerization to achieve high selectivity. By our method we obtained the synthesis of *E*-stilbenes bearing one, two or three methoxy groups at one of the aryl rings and different boron-containing functional group at different position of the second ring. The borylated stilbenes showed interaction with a single binding site on HSA, with the boronic ester and benzoxaborole derivatives binding through hydrophobic interactions, while the boronic acid derivative bound *via* electrostatic forces.

Conflicts of interest

There are no conflicts to declare.

Data availability

The data and materials necessary to reproduce the findings reported in this manuscript are available upon request to the corresponding author.

Supplementary information: full experimental details and copies of NMR spectra. See DOI: <https://doi.org/10.1039/d5ra05162b>.

Acknowledgements

We are grateful to CNPq, CAPES (Financial code 001), and INCT-Catalise for financial support.

References

- 1 F. Kratz, *J. Control. Release*, 2008, **132**, 171; D. Sleep, *Exp. Opin. Drug Deliv.*, 2015, **12**, 793; G. Fanali, A. Masi, V. Trezza, M. Marino, M. Fasano and P. Ascenzi, *Mol. Aspects Med.*, 2012, **33**, 209.
- 2 F. Samari, M. Shamsipur, B. Hemmateenejad and T. Khayamian, *Eur. J. Med. Chem.*, 2012, **54**, 255; J. R. Simard, P. A. Zunszain, C. E. Ha, J. S. Yang, N. V. Bhagavan, I. Petitpas, S. Curry and J. A. Hamilton, *Proc. Natl. Acad. Sci. U. S. A.*, 2005, **102**, 17958; J. R. Simard, P. A. Zunszain, J. A. Hamilton and S. Curry, *J. Mol. Biol.*, 2006, 361–336; O. K. Abou-Zied and O. I. K. Al-Shihi, *J. Am. Chem. Soc.*, 2008, **130**, 10793.
- 3 R. E. Olson and D. Christ, *Annu. Rep. Med. Chem.*, 1996, **31**, 327; S. Schmidt, D. Gonzalez and H. Derendorf, *J. Pharm. Sci.*, 2010, **99**, 1107; A. Varshney, P. Sen, E. Ahmad, M. Rehan, N. Subbarao and R. H. Khan, *Chirality*, 2010, **22**, 77.
- 4 Y. Wang, F. Catana, Y. Yang, R. Roderick and R. B. B. Van, *J. Agric. Food Chem.*, 2002, **50**, 431.
- 5 J. A. Baur, K. J. Pearson, N. L. Price, H. A. Jamieson, C. Lerin, A. Kalra, V. V. Prabhu, J. S. Allard, G. Lopez-Lluch, K. Lewis, P. J. Pistell, S. Poosala, K. G. Becker, O. Boss, D. Gwinn, M. Wang, S. Ramaswamy, K. W. Fishbein, R. G. Spencer, E. G. Lakatta, D. L. Couteur, R. J. Shaw, P. Navas, P. Puigserver, D. K. Ingram, R. de Cabo and D. A. Sinclair, *Nature*, 2006, **444**, 337; N. M. O. Arcanjo, C. Luna, M. S. Madruga and M. Estévez, *Biochim. Biophys. Acta, Gen. Subj.*, 2008, **1862**, 1938; B. Jannin, M. Menzel, J. P. Berlot, D. Delmas, A. Lançon and N. Latruffe, *Biochem. Pharmacol.*, 2004, **68**, 1113.
- 6 Y. Fan, Y. Liu, L. Gao, Y. Zhang and J. Yi, *Food Chem.*, 2018, **261**, 283; M. Pantusa, R. Bartucci and B. Rizzuti, *J. Agricultural Food Chem.*, 2014, 62–64384; Z. Lu, Y. Zhang, H. Liu, J. Yuan, Z. Zheng and G. Zou, *J. Fluoresc.*, 2007, **17**, 580.
- 7 M. Karimi, S. Bahrami, S. B. Ravari, P. S. Zangabad, H. Mirshekari, M. Bozorgomid and M. R. Hamblin, *Expert Opin. Drug Deliv.*, 2016, **13**, 1609; X. Liu, Y. Shang, X. Ren and H. Li, *J. Chem.*, 2013, **1**; S. Cao, D. Wang, X. Tan and J. Solut, *Chem*, 2009, **38**, 1193.
- 8 D. J. Boocock, G. E. S. Faust, K. R. Patel, A. M. Schinas, V. A. Brown, M. P. Ducharme, T. D. Booth, J. A. Crowell, M. Perloff, A. J. Gescher, W. P. Steward and D. E. Brenner, *Cancer Epidemiol., Biomarkers Prev.*, 2007, **16**, 1246; J. P. Rezende, E. A. Hudson, H. M. C. Paula, R. S. Meinel,



- A. D. Silva, L. H. M. Silva and A. C. S. Pires, *Food Chem.*, 2020, **307**, 125514.
- 9 S. Sale, R. D. Verschoyle, D. Boocock, D. J. L. Jones, N. Wilsher, K. C. Ruparelia, W. P. Steward and A. J. Gescher, *Br. J. Cancer*, 2004, **90**, 736; G. A. Potter, P. C. Butler, K. C. Ruparelia, T. Ijaz, N. Wilsher, E. Wanogho, H. L. Tan, T. T. V. Hoang, L. A. Stanley and M. D. Burke, *Br. J. Cancer*, 2002, **86**, S117; S. Sale, R. G. Tunstall, K. C. Ruparelia, G. A. Potter, W. P. Steward and A. J. Gescher, *Int. J. Cancer*, 2005, **115**, 194; Z. Ma, O. Molavi, A. Haddadi, R. Lai, R. A. Gossage and A. Lavasanifar, *Cancer Chemother. Pharmacol.*, 2008, **63**, 27; H. Piotrowska-Kempisty, M. Ruciński, S. Borys, M. Kucińska, M. Kaczmarek, P. Zawierucha, M. Wierzchowski, D. Łażewski, M. Murias and J. Jodynis-Liebert, *Sci. Rep.*, 2016, **6**, 32627.
- 10 K. Messner, B. Vuong and G. K. Tranmer, *Pharmaceuticals*, 2022, **15**, 264.
- 11 Z. A. Khan, A. Iqbal and S. A. Shahzad, *Mol. Divers.*, 2017, **21**, 483.
- 12 B. C. Das, S. M. Mahalingam and T. Evans, *Tetrahedron Lett.*, 2009, **50**, 3031; B. C. Das, X. Zhao, X. Tang and F. Yang, *Bioorg. Med. Chem. Lett.*, 2011, **21**, 5638; V. M. Yenugonda, Y. Kong, T. B. Deb, Y. Yang, R. B. Riggins and M. L. Brown, *Cancer Biol. Ther.*, 2012, **13**, 925; B. C. Das, S. M. Mahalingam, S. Das, N. S. Hosmane and T. Evans, *J. Organom. Chem.*, 2015, **798**, 51; A. Oehlke, A. A. Auer, I. Jahre, B. Walfort, T. Ruffer, P. Zoufala, H. Lang and S. Spange, *J. Org. Chem.*, 2007, **72**, 4328.
- 13 J. S. Costa, R. K. Braun, P. A. Horn, D. S. Lüdtke and A. V. Moro, *RSC Adv.*, 2016, **6**, 59935; M. E. Contreira, D. S. Lüdtke and A. V. Moro, *Tetrahedron Lett.*, 2018, 59–2784; L. L. Baldassari, E. A. Cechinatto and A. V. Moro, *Green Chem.*, 2019, 21–3556; L. L. Baldassari, K. S. Santos, C. P. Ebersol, D. S. Lüdtke and A. V. Moro, *Catal. Sci. Technol.*, 2020, 10–7476; H. C. Zimba, L. L. Baldassari and A. V. Moro, *Org. Biomol. Chem.*, 2022, 20–6239; E. O. Boeira, C. B. Plá, F. S. Rodembusch and A. V. Moro, *ChemCatChem*, 2023, **15**, e202201355.
- 14 T. Ismail, S. Shafi, J. Srinivas, D. Sarkar, Y. Qurishi, J. Khazir, M. S. Alam and H. M. S. Kumar, *Bioorg. Chem.*, 2016, **64**, 97.
- 15 J. Wu, D. Li and D. Zhang, *Synth. Commun.*, 2005, **35**, 2543.
- 16 P. Klumphu and B. H. Lipshutz, *J. Org. Chem.*, 2014, **79**, 888.
- 17 B. H. Lipshutz, S. Ghorai, A. R. Abela, R. M. Moser, T. Nishikata, C. Duplais, A. Krasovskiy, R. D. Gaston and R. C. Gadwood, *J. Org. Chem.*, 2011, **76**, 4379.
- 18 R. Starosta, F. C. Santos and R. F. M de Almeida, *J. Mol. Struct.*, 2020, **1221**, 128805.
- 19 G. Sudlow, D. J. Birkett and D. N. Wade, *Mol. Pharmacol.*, 1975, **11**, 824.
- 20 G. Sudlow, D. J. Birkett and D. N. Wade, *Mol. Pharmacol.*, 1976, **12**, 1052–1061.
- 21 K. Yamasaki, V. T. G. Chuang, T. Maruyama and M. Otagiri, *Biochim. Biophys. Acta, Gen. Subj.*, 2013, **1830**, 5435.
- 22 K. L. Fraiji, D. M. Hayes and T. C. Werner, *J. Chem. Educ.*, 1992, **69**, 424.
- 23 P. D Ross and S. Subramanian, *Biochemistry*, 1981, **20**, 3096.
- 24 M. A. Martínez-Aguirre, M. F. Alamo, K. E. Trejo-Huizar and A. K. Yatsimirsky, *Bioorg. Chem.*, 2021, **113**, 104993.

